Effects of Inertial Confinement on the Ignition of Diffusion-Free Unreacted Pockets

Jonathan D. Regele
Iowa State University
Ames, IA, USA

1 Introduction

Volumes of unreacted fluid surrounded by combustion products are observed in Deflagration-to-Detonation Transition (DDT) [1] and unstable cellular detonations [2]. These pockets form behind the slip line after being preheated by the incident shock and take the shape of a tongue. The region of unreacted fluid becomes a completely isolated pocket once the incident shock reflects off a wall and becomes a Mach shock or the incident shock encounters another Mach shock [2].

Unburned pocket formation is typical of reactive mixtures with large activation energies, such as methane and oxygen, where the activation energy is estimated to be $E'_a \approx 36\,\mathrm{kcal/mol}$ [2, 3]. Transport effects can influence the consumption of reactant within these pockets. In particular diffusion plays a major role when activation energies are large and the induction period of the unreacted pocket is long [2]. In contrast, diffusion can play a minor role when reactive mixtures have small to moderately large activation energies because the reaction time of the shocked gas behind the incident shock is short. Similar phenomena are observed in indirect detonation initiation where heat is added to a localized volume of fluid on the acoustic timescale [4, 5].

Several different scales are involved in the consumption of unreacted pockets including the ignition delay, reaction, diffusion, and acoustic times. The current work focuses on the limit when diffusion effects are negligible and examines the dependence of delay time on initial size.

Kassoy showed for an inert gas that if a spatially resolved volume of fluid is heated over a timescale much shorter or longer than the acoustic timescale associated with the fluid volume that nearly constant volume or constant pressure heat addition occurs, respectively [6]. In this work, the reactive Euler equations are used to simulate one-dimensional unreacted pockets of different sizes. It is demonstrated that the acoustic timescale associated with the size of the pocket can be used to distinguish between pockets that react at nearly constant pressure and constant volume conditions, and any conditions that occur between these two extremes.

2 Modeling Approach

The nondimensional reactive Euler equations are solved in one dimension with the hyperbolic solver developed for the adaptive wavelet-collocation method [7]. A simple one-step Arrhenius reaction rate is

Correspondence to: jregele@iastate.edu

used for the chemical reaction. Thus the governing equations are expressed

$$\frac{\partial \rho}{\partial t} + \frac{\partial \rho u}{\partial x} = 0 \tag{1a}$$

$$\frac{\partial \rho u}{\partial t} + \frac{\partial}{\partial x}(\rho u^2 + p) = 0 \tag{1b}$$

$$\frac{\partial \rho e_T}{\partial t} + \frac{\partial}{\partial x}(\rho e_T + p)u = 0 \tag{1c}$$

$$\frac{\partial \rho Y}{\partial t} + \frac{\partial \rho Y u}{\partial x} = -\dot{\omega}\,. \tag{1d}$$

The non-dimensionalized equation of state and reaction rate are defined

$$p = (\gamma - 1)\left(\rho e_T - \frac{1}{2}\rho u^2 - \rho Y q\right) \tag{2}$$

$$\dot{\omega} = B\rho Y \exp(-E_a/T), \tag{3}$$

where Y is the mass fraction of the reactants, and q is the heat of reaction. The reaction rate $\dot{\omega}$ contains the pre-exponential factor B and the activation energy E_a. In addition to the fuel species equation, an additional species equation (Y_t) is solved with a zero source term to track the location of the burnt/unburnt gas interface for the entire duration of the simulation.

The nondimensional variables shown above are defined with respect to a reference state and an arbitrary length scale l' such that $\rho = \rho'/\rho'_0$, $u = u'/a'_0$, $t = t'a'_0/l'$, $p = p'/\rho'_0 a'^2_o$, $e = e'/a'^2_0$, $T = T'/\gamma T'_0$, where primes indicate dimensioned quantities and the subscript 0 denotes the reference state. The pre-exponential, activation energy, and heat of reaction are nondimensionalized $B = B'l'/a'_0$, $E_a = E'_a/a'^2_0$, and $q = q'/a'^2_0$, respectively. With this nondimensionalization the temperature is related to pressure and density by $T = p/\rho$.

3 Problem Statement

Although the motivation of the current work is based upon the observance of unreacted pockets in unstable and mildly unstable detonations where the non-dimensional activation energies are high $E_a \approx 60$ [2]. The primary objective is to classify a hot spot's behavior using acoustic timescale theory [6] between two limiting extremes, isobaric and isochoric ignition. Thus, as it is shown in the following work, it is not necessary to use large activation energies in order to capture the range of behaviors that may be observed inside these pockets.

The reactive fluid is characterized by the heat of reaction $q = 42$, specific heat ratio $\gamma = 1.2$, a modest activation energy $E_a = 17$, and a pre-exponential factor $B = 10$. These conditions are similar to that used in the moderately unstable case in Ref. [3]. The initial state of the reactive pocket is $p_p = 5$ and $\rho_p = 1$. The fluid is initially at rest. Symmetry conditions are used at the origin and transmissive conditions on the right.

A calculation of the homogeneous constant volume and constant pressure half-reaction times give $\tau_v = 0.829$ and $\tau_p = 0.915$. The speed of sound $a = \sqrt{\gamma T}$ inside the pocket can be used to define a length scale associated with the reaction timescale $L = \tau_v\sqrt{\gamma T_p} = 2.0$. Three different cases are performed with the same initial state where the pocket sizes are $l = L/10 = 0.2$, $l = 10L = 20$, and $l = L = 2$. These correspond to acoustic to reaction timescale ratios of $t_a/\tau_v = 0.1$, 10, and 1, respectively. The computational domain spans $x \in [0, 5l]$ with the unreacted pocket of length l centered at the origin. The initial pressure $p = 5$ is uniform through the domain and the initial burnt fluid temperature outside the unreacted pocket is prescribed assuming constant pressure combustion occurred so that $T_b = T_p + (\gamma - 1)q/\gamma = 12$.

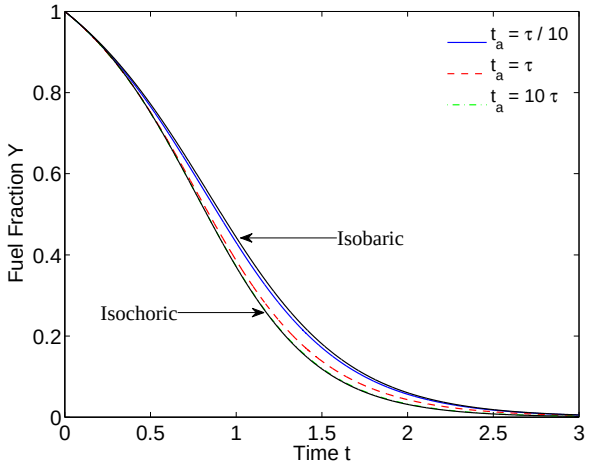

Figure 1: Fuel Mass fraction as a function of time for the three different cases are compared to the constant volume and constant pressure curves.

4 Results

It can be anticipated that when the acoustic timescale of the unreacted pocket is much less than the reaction timescale constant pressure combustion will occur. On the other hand, if the pocket's acoustic timescale is much larger than the reaction timescale, the fluid will be inertially confined and a constant volume combustion process will occur. The three cases presented here demonstrate what occurs between these two extremes. For convenience the following naming convention will be used. The case with $t_a/\tau_v = 0.1$ will be referred to as the "unconfined" case, $t_a/\tau_v = 10$ the "confined" case, and $t_a/\tau_v = 1$ the "partially confined" case.

Figure 1 plots the fuel fraction for the three cases as a function of time. The fuel fraction for the isobaric and isochoric combustion processes are plotted for reference. The isobaric and isochoric autoignition times differ by only 10%. As can be expected, the three different cases lie between the two limiting extreme cases. The unconfined case lies close to the isobaric curve, the confined case close to the isochoric, and the partially confined case between each of those.

Figures 2, 3, and 4 plot the (a) fuel mass fraction and (b) pressure on x-t diagrams for the unconfined, confined, and partially confined cases, respectively. Superimposed in each figure are lines indicating the acoustic and reaction timescales. An additional vertical line indicates the tracking fluid interface where $Y_t = 0.5$.

It can be seen from Fig. 2(a) that the amount of fuel consumed during the acoustic time in the unconfined case is small. The pressure in Fig. 2(b) shows that compression waves are generated from the reaction and that the original burnt/unburnt gas interface moves a distance on the order of the original pocket size l or more during the entire reaction time. Furthermore, the pressure contour shows that the pressure rises by only 4% during the reaction duration. This indicates that the combustion process in the unconfined case is nearly a constant pressure process.

Figure 3 plots x-t diagrams for the confined case. The fuel mass fraction plot shows that a majority of the fuel is consumed in the reaction time τ_v. The burnt/unburnt gas interface moves little if any during the reaction timescale. The pressure plot shows a rapid rise in pressure, as would be expected with a nearly constant volume combustion process. The pressure rises to a peak value of 12 during the reaction time τ_v, which creates a strong compression wave which becomes a full shock. An expansion fan is generated simultaneously with the shock and reaches the origin at roughly the acoustic time. The

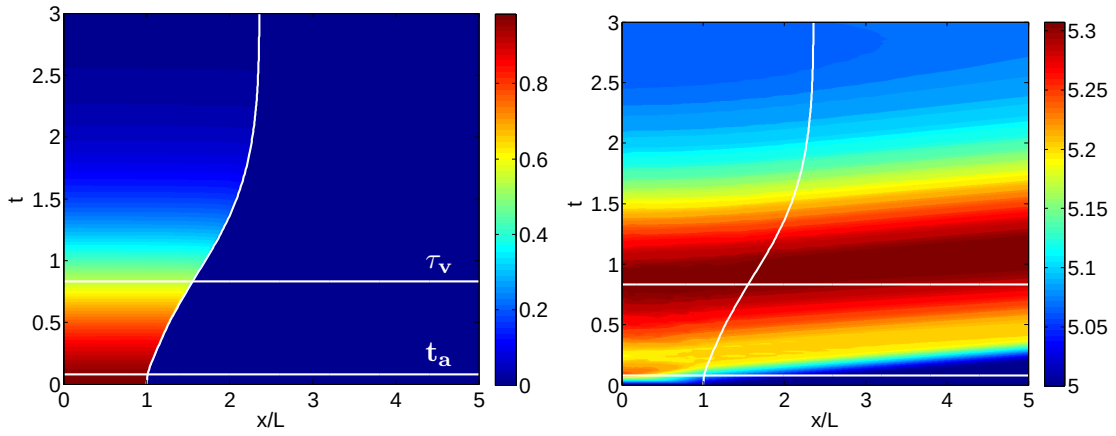

(a) Fuel Mass Fraction Y (b) Pressure p

Figure 2: x-t contour plots for (a) the fuel mass fraction Y and (b) pressure p are plotted for the unconfined case.

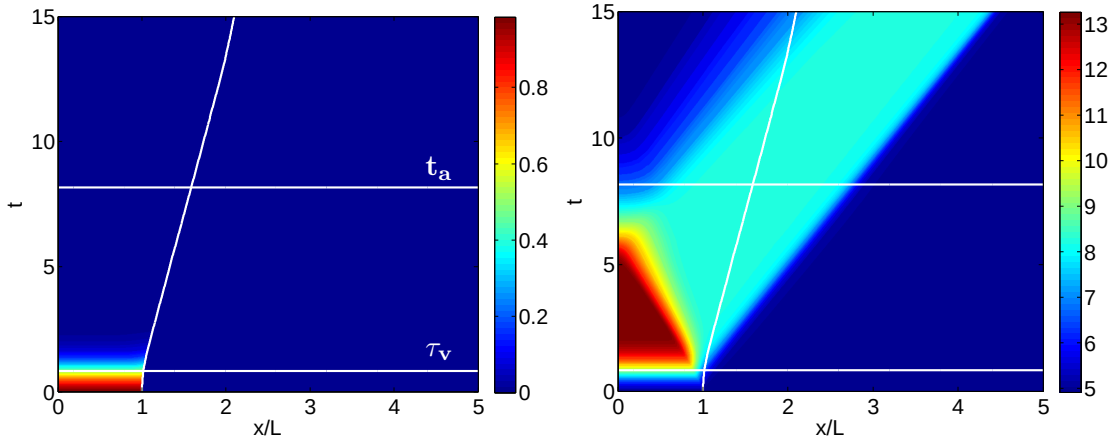

(a) Fuel Mass Fraction Y (b) Pressure p

Figure 3: x-t contour plots for (a) the fuel mass fraction Y and (b) pressure p are plotted for the confined case.

expansion wave is reflected at the origin and follows behind the shock wave for $t > t_a$. The vertical line demarcating the burnt/unburnt gas interface has a constant slope. This indicates that the induced fluid velocity is relatively constant until the expansion wave reaches the contact location and brings the fluid to rest.

The x-t diagrams for the partially confined case are shown in Fig. 4. In this case the reaction and acoustic timescales are equal and simultaneous gas expansion and compression will occur during the reaction time. Figure 4(a) shows the burnt/unburnt gas interface moves approximately 10% of the original pocket size during the reaction timescale. In Fig. 4(b), compression waves are generated simultaneously with the expansion wave. The pressure inside the pocket continues to increase until the expansion wave reaches the pocket center. Once the expansion wave has reached the pocket center the pressure begins to drop and a finite compression wave propagates away from the origin. The amplitude of the compression wave is only slightly less than that of the shock wave in the confined case.

Figure 5 plots the mean and center pocket pressures for each of the three cases. For reference, the isobaric $p = 5$ and isochoric pressure curves are plotted as well. The unconfined case rises by only 4%

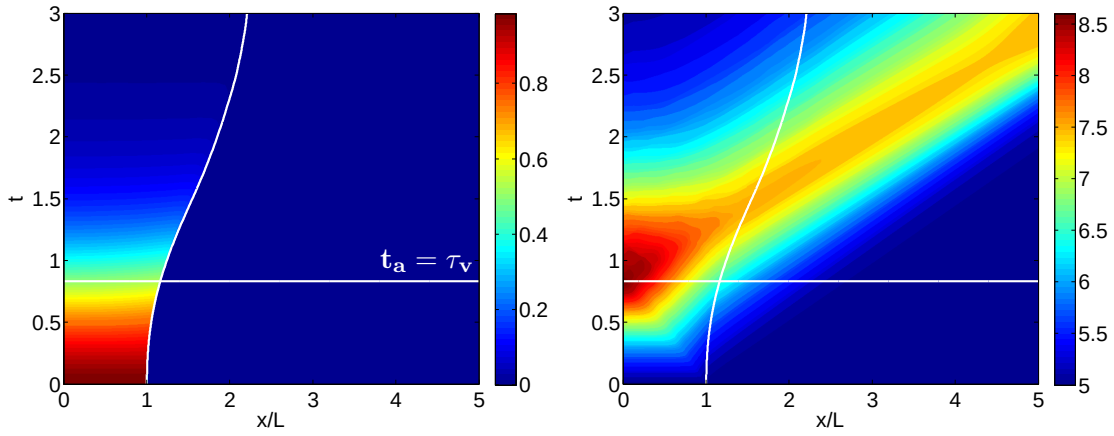

(a) Fuel Mass Fraction Y (b) Pressure p

Figure 4: x-t contour plots for (a) the fuel mass fraction Y and (b) pressure p are plotted for the partially confined case.

above the initial pressure $p = 5$ for both the mean and center pressures. For the confined case, Fig. 5(a) shows that the mean pocket pressure rises synonymously with with the isochoric bounding curve for over half the reaction duration. Furthermore, the center pressure for the confined case is exactly equal to the isochoric curve until the the expansion wave reaches the pocket center.

The partially confined case shows essentially what the name describes, a partially confined combustion process. The mean pocket pressure rises similar to the isochoric curve for a short time, but then deviates and reaches a maximum shortly after the acoustic/reaction time. The center pressure does rise exactly with the isochoric curve until the expansion wave reaches the pocket center at roughly the acoustic time. The pressure for both the mean and pocket center tends toward the starting pressure $p = 5$ as the reaction completes. Although the magnitude of the compression wave generated in the partially confined case is nearly equal to that of the shock wave in the confined case, the mean and center pressures attained during the reaction fall short of the confined case pressures by more than 50%.

5 Conclusions

It is demonstrated that the half-reaction time is a small function of the volumetric dimension of the fluid. The half-reaction time lies on a continuum scale with the isobaric and isochoric half-reaction times demarcating the limits. While the half-reaction time varies only slightly on the pocket size, the gasdynamic response varies greatly over a range of pocket lengths spanning only two orders of magnitude.

The acoustic timescale is used to characterize the impact of the pocket's reaction on the surrounding fluid. If the acoustic time is $1/10^{\text{th}}$ of the reaction timescale the pocket is consumed in a nearly constant pressure combustion process. In the opposite case where the acoustic time is 10 times the reaction timescale the fluid is inertially confined and is consumed in a nearly constant volume process. If the two scales are equal, the pressure rises simultaneously as the fluid expands and a finite compression wave is emitted away from the pocket center. Thus, if the size and temperature of an unreacted pocket are known, a simple ratio of the acoustic and reaction timescales can be used to estimate the impact of the pocket's reaction on the surrounding fluid. Although the current analysis examines a relatively small activation energy, the methodology can be easily extended to higher activation energy mixtures.

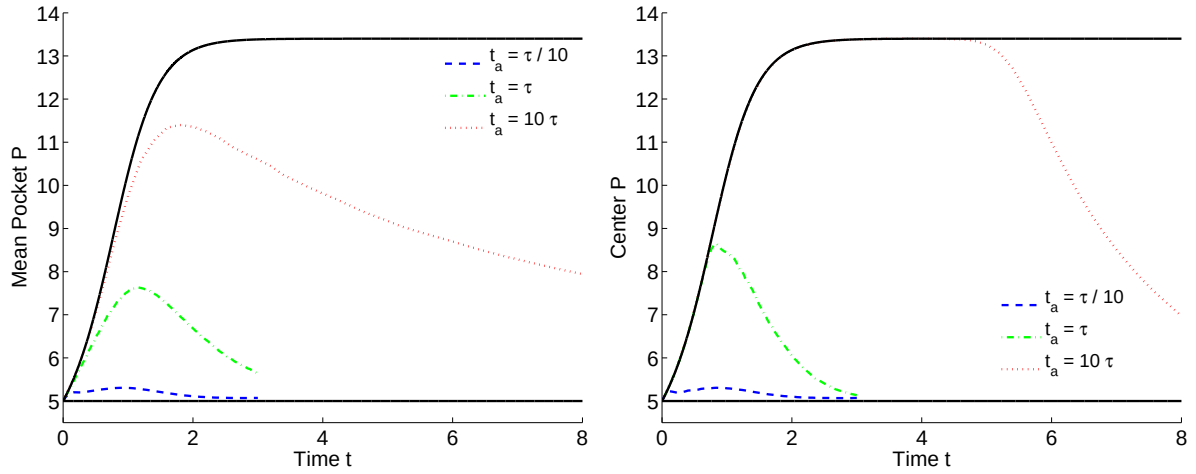

(a) Mean pocket pressure $\bar{p}$ (b) Pocket Center pressure

Figure 5: The (a) mean pocket and (b) centerline pressure are plotted as a function of time for the three different cases. The isobaric $p = 5$ and isochoric curves are plotted for comparison.

References

[1] Oran E S and Gamezo V N, (2007). Origins of the deflagration-to-detonation transition in gas-phase combustion. *Combust. Flame*, 148.

[2] Radulescu M. I. Sharpe G. J. Law C. K. and Lee J. H. S. (2007). The hydrodynamic structure of unstable cellular detonations. *J. Fluid Mech.* 580.

[3] Mazaheri K, Mahmoudi Y, and Radulescu M I. (2012). Diffusion and hydrodynamic instabilities in gaseous detonations. *Combust. Flame*, 159.

[4] Kassoy D. R., Kuehn J. A., Nabity M. W., and Clarke J. F. (2008). Detonation initiation on the microsecond time scale: DDTs. *Combust. Theory Mod.* 12.

[5] Regele J. D., Kassoy D. R., and Vasilyev O. V. (2012). Effects of high activation energies on acoustic timescale detonation initiation. *Combust. Theory and Mod.* 16.

[6] Kassoy D. R. (2010). The response of a compressible gas to extremely rapid transient, spatially resolved energy addition: an asymptotic formulation. *J. Eng. Math.* 68.

[7] Regele J. D. and Vasilyev O. V. (2009). An Adaptive Wavelet-Collocation Method for Shock Computations. *Intl. J. of Comp. Fluid Dynamics*. 23:7.